Analytic Differential Admittance Operator Solution of a Dielectric Sphere under Radial Dipole Illumination

M. Huynen[#1], D. De Zutter[#2], D. Vande Ginste[#3], V. Okhmatovski[*4]

[#]quest, IDLab, Department of Information Technology, Ghent University/imec, Ghent, Belgium

[*]Department of Electrical and Computer Engineering, University of Manitoba, Winnipeg, Canada

[1]martijn.huynen@ugent.be, [2]daniel.dezutter@ugent.be, [3]dries.vandeginste@ugent.be, [4]vladimir.okhmatovski@umanitoba.ca

***Abstract*— In this contribution, the exact solution of the electric field integral equation (EFIE) combined with the differential surface admittance (DSA) operator is presented for scattering at a homogeneous dielectric sphere. By employing a Galerkin Method of Moments with two complete sets of orthogonal vector spherical harmonics as basis functions, both operators involved are constructed with closed expressions. By comparing to the classic Mie series solution for illumination by a radial electric dipole, the DSA-EFIE approach is confirmed to yield the exact solution within 12 digits of accuracy.**

***Keywords*— integral equations, method of moments, single-source, differential-surface admittance.**

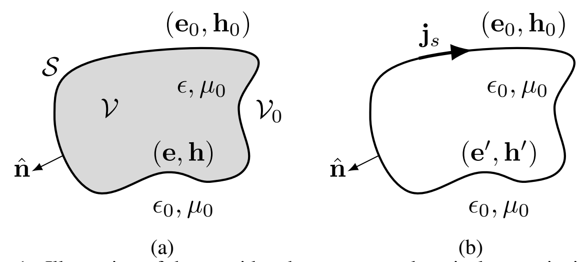

Fig. 1. Illustration of the considered geometry and equivalence principle with (a) the original situation and (b) the single-source equivalence.

I. Introduction

The differential surface admittance (DSA) operator is one of the many techniques developed over the decades to tackle the issue of accurate broadband modeling for a wide variety of materials. The central approach in DSA-based methods consists of the application of the single source equivalence principle to impose a fictitious current density on the boundary that preserves field quantities on the outside. The fictitious current itself is consequently expressed as an operator, computed via the volume's eigenmodes [1], the Fokas method [2] or through the replaced medium's Greens function [3], acting on the boundary electric field. Uniquely, the first two approaches circumvent the need for the sometimes challenging numerical integration of medium's Greens function, e.g., for good conductors in skin effect regime [4], while the third path can rely on well-established routines to overcome potential hurdles.

First established for 2-D rectangular and circular cross-sections [1], the method has seen its fair share of development over the last 20 years, including extensions to other shapes such as triangles and polygons [5], the inclusion of semiconductors and magnetic materials [6], alternative approaches to obtain the matrix form of the operator [2], [3], and the development of a 3-D equivalent for cylinders and cuboids [7], [8]. Although the various publications and incarnations of the DSA approach have shown excellent accuracy, competitive computation times and diverse application opportunities, some fundamental questions about the eigenmode-based computation approach remain in terms of frequency-dependent properties, convergence and rigor.

Thereto, we start the analysis of these properties in this paper by following the approach proposed in [9], [10], which look at scattering by PEC and homogeneous dielectric spheres, respectively, using the Galerkin Method of Moments, employing vector spherical harmonics as test and basis functions. By decomposing both the electric field integral equation (EFIE) and the DSA operators, which handle the outside and inside region, respectively, in terms of these harmonics as well, all inner products involved in the Galerkin technique can be evaluated analytically; hence, establishing an exact analytic solution of the DSA-EFIE for a dielectric sphere. The closed expressions are found for all relevant field quantities and compared to the classical Mie series solution.

II. The differential surface admittance operator

Take a homogeneous dielectric object $\mathcal{V}$ with (complex) relative permittivity ϵ and permeability μ_0 as shown in Figure 1a. According to the single-source equivalence theorem [11], the material inside $\mathcal{V}$ can be replaced by the background medium, with parameters ϵ and μ_0, by imposing a surface current density $\mathbf{j}_s$ on the boundary $\mathcal{S}$ (see Figure 1b). The fields outside then remain the same and are given by the electric field integral equation:

$$\hat{\mathbf{n}}\times\mathbf{e}_0^t(\mathbf{r}) = \hat{\mathbf{n}}\times\mathbf{e}_{\text{inc}}(\mathbf{r}) + \mathcal{T}\circ\mathbf{j}_s \qquad \mathbf{r}\in\mathcal{S}, \quad (1)$$

$$= \hat{\mathbf{n}}\times\mathbf{e}_{\text{inc}} - j\omega\mu_0\hat{\mathbf{n}}\times\int_{\mathcal{S}}\overline{\overline{G}}(|\mathbf{r}-\mathbf{r}'|)\mathbf{j}_s(\mathbf{r}')\,\mathrm{d}\mathbf{r}', \quad (2)$$

with $\mathbf{e}_0^t$ the tangential component of the electric field at $\mathcal{S}$, $\mathbf{e}_{\text{inc}}$ the incoming field, $\mathcal{T}$ the EFIE operator and $\overline{\overline{G}}$ the Green's dyadic of the background medium. An expression for the (presently) unknown surface current density $\mathbf{j}_s$ is obtained by means of the DSA operator. In this contribution, we will focus on the 3-D expansion of its original form [7]:

$$\mathbf{j}_s(\mathbf{r}) = \mathcal{Y} \circ \mathbf{e}_0^t \qquad \mathbf{r} \in \mathcal{S}, \tag{3}$$

$$= -\eta \sum_\nu \left[\frac{\mathcal{K}_\nu}{\mathcal{N}_\nu^2} \int_{\mathcal{S}} (\hat{\mathbf{n}} \times \mathbf{h}_\nu^*(\mathbf{r}')) \cdot \mathbf{e}_0^t(\mathbf{r}')\, \mathrm{d}\mathbf{r}' \right] (\hat{\mathbf{n}} \times \mathbf{h}_\nu(\mathbf{r})), \tag{4}$$

with $\mathcal{Y}$ the DSA operator, k_0 and k the wavenumber of the background medium and the volume's medium, respectively, η the contrast parameter $(k^2 - k_0^2)/(j\omega\mu_0)$, $\mathcal{K}_\nu$ a shorthand for $k_\nu^2/[(k_\nu^2 - k^2)(k_\nu^2 - k_0^2)]$, and $\mathbf{h}_\nu$ the magnetic eigenmode of a cavity with perfect electric conducting walls in the shape of $\mathcal{V}$ filled by the background medium with k_ν its wavenumber and $\mathcal{N}_\nu$ its normalization constant.

III. Galerking MoM on a Sphere

A. Expansion into basis functions

To analyze the specific configuration of a dielectric sphere, we follow the Helmholtz decomposition procedure and notation put forward in [10] to expand the unknown surface quantities $\mathbf{j}_s$ and $\mathbf{e}_0^t$ as

$$\mathbf{j}_s = \sum_{n'=0}^{N} \sum_{m'=-n'}^{n'} \alpha_{n'm'}^{(1)} \mathbf{u}_{n'm'}^{(1)} + \alpha_{n'm'}^{(2)} \mathbf{u}_{n'm'}^{(2)}, \tag{5}$$

$$\mathbf{e}_0^t = \sum_{n''=0}^{N} \sum_{m''=-n''}^{n''} \beta_{n''m''}^{(1)} \mathbf{u}_{n''m''}^{(1)} + \beta_{n''m''}^{(2)} \mathbf{u}_{n''m''}^{(2)}, \tag{6}$$

with $\mathbf{u}_{nm}^{(1)}$ and $\mathbf{u}_{nm}^{(2)}$ two sets of orthogonal, complete sets of vector basis function defined on the surface of a sphere with radius a as

$$\mathbf{u}_{nm}^{(1)}(\theta, \phi) = \sqrt{d_{nm}} \nabla^t Y_n^m(\theta, \phi), \tag{7}$$

$$\mathbf{u}_{nm}^{(2)}(\theta, \phi) = \sqrt{d_{nm}} \hat{\mathbf{r}} \times \nabla^t Y_n^m(\theta, \phi). \tag{8}$$

The exact definition and corresponding normalization choice of the scalar spherical harmonics Y_n^m and their normalization constant d_{nm} can be found in [10].

The Green's dyadic in (1) can be expanded over vector spherical harmonic functions as well:

$$\overline{\overline{G}}(\mathbf{r}, \mathbf{r}') = -jk_0 \sum_{n,m} d_{nm} \cdot \begin{cases} \mathbf{p}_{n,m}^{(1)}(\mathbf{r})\, \mathbf{p}_{n,-m}^{(2)}(\mathbf{r}') + \mathbf{q}_{n,m}^{(1)}(\mathbf{r})\, \mathbf{q}_{n,-m}^{(2)}(\mathbf{r}'), & r < r' \\ \mathbf{p}_{n,m}^{(2)}(\mathbf{r})\, \mathbf{p}_{n,-m}^{(1)}(\mathbf{r}') + \mathbf{q}_{n,m}^{(2)}(\mathbf{r})\, \mathbf{q}_{n,-m}^{(1)}(\mathbf{r}'), & r > r' \end{cases}, \tag{9}$$

with $\mathbf{p}^{(j)}$ and $\mathbf{q}^{(j)}$ defined as in (21)-(22) in [10]. The relevant magnetic eigenmodes $\mathbf{h}_\nu$ for a nonmagnetic sphere can be found in [12] and belong to two distinct classes, i.e., transversal magnetic ($\mathrm{TM_r}$) and transversal electric ($\mathrm{TE_r}$) eigenmodes, which are defined as:

$$\mathbf{h}_{nms}^{\mathrm{TM}} = \nabla \times [r j_n(k_{ns} r) Y_n^m(\theta, \phi)\, \hat{\mathbf{r}}] \tag{10}$$

$$\mathbf{h}_{nms}^{\mathrm{TE}} = \frac{1}{\kappa_{ns}} \nabla \times \nabla \times [r j_n(\kappa_{ns} r) Y_n^m(\theta, \phi)\, \hat{\mathbf{r}}], \tag{11}$$

where $j_n(x)$ is the spherical Bessel function, $k_{ns} = x_{ns}/a$ with x_{ns} the roots of $[xj_n(x)]' = 0$, and $\kappa_{ns} = y_{ns}/a$ with y_{ns} the roots of $j_n(x) = 0$.

B. Radial dipole illumination

In this contribution, we limit ourselves to one particular excitation, viz., a radial dipole. This source aligned along the z-axis with dipole moment $1\,\mathrm{A{\cdot}m}$ is placed on the z-axis at a distance r_0 from the origin, which is also the center of the sphere. In this configuration, the solution will be independent of ϕ due to circular symmetry in the azimuth plane. Moreover, it can be shown [10] that only $\mathrm{TM_r}$ waves are present in this set-up and that only the basis functions $\mathbf{u}^{(1)}$ are required in this solution, greatly simplifying the analysis in the remainder of this work.

Turning our attention first to the EFIE (1), we will discretize (1) into a matrix equation by substituting (5) and (6) and testing both sides with $\mathbf{u}_{nm}^{(1)\,*}$. Fully making use of the orthogonality of the spherical harmonics ((72)-(75) in [9]), it is shown that every individual $\mathbf{u}_{n'm}^{(1)}$ in (5) maps onto only its counterpart in (6). As such, the discretized equation is given by

$$\beta_{nm}^{(1)} = \gamma_{nm} + \mathcal{Z}_{nm}^{2,1} \alpha_{nm}^{(1)}, \tag{12}$$

with γ_{nm} and $\mathcal{Z}^{2,1}$ given by (96) and (35) in [10] (see details of the derivation therein), respectively:

$$\gamma_{nm} = -\omega\mu_0 \sqrt{d_{nm}} \frac{n(n+1)}{k_0 r_0} h_n^{(2)}(k_0 r_0) [k_0 a j_n(k_0 a)]' \delta_{m,0}, \tag{13}$$

$$\mathcal{Z}_{nm}^{2,1} = -\frac{\omega\mu_0}{k_0} [k_0 a h_n^{(2)}(k_0 a)]' [k_0 a j_n(k_0 a)]', \tag{14}$$

with $[xz_n(x)]'$ a shorthand for $z_n(x) + xz_n'(x)$.

The discretization strategy for the DSA operator follows the same blueprint. Fortunately, we can rely once again on the same properties of the orthogonal spherical harmonics since (10) is of the same form as $\mathbf{p}^{(1)}$, albeit with k replaced by k_{ns}. Introducing the closed form expression for the normalization constant of the TM eigenmodes (10) (see (A9.22) in [12]), we find the following relation

$$\alpha_{nm}^{(1)} = \mathcal{Y}_{nm}^{1,1} \beta_{nm}^{(1)}, \tag{15}$$

with

$$\mathcal{Y}_{nm}^{1,1} = \frac{-1}{j\omega\mu_0 a} \sum_{s=1}^{\infty} \frac{2k_{ns}^2 \left(k^2 - k_0^2\right)}{(k_{ns}^2 - k^2)(k_{ns}^2 - k_0^2)\left[1 - \frac{n(n+1)}{x_{ns}^2}\right]}. \tag{16}$$

C. Generalized Fourier series

Evaluating (16) with a high level of accuracy is challenging as the summation can be slow to converge and requires the roots x_{ns}. Propitiously, a closed sum for this series was obtained through the application of the generalized Fourier series concept, in particular an adaptation of the Fourier-Bessel expansion [13]. For the application at hand, it states that a square-integrable function on the interval $[0, a]$ can be expanded as

$$f(r) = \sum_{s=1}^{\infty} c_s\, j_n(k_{ns} r) = \sum_{s=1}^{\infty} \frac{\langle f, j_n(k_{ns} r)\rangle}{||j_n(k_{ns} r)||^2} j_n(k_{ns} r), \quad (17)$$

with $\langle f, g\rangle = \int_0^a f(r) g(r) r^2\, \mathrm{d}r$. When we apply this expansion for the following function:

$$f(r) = \frac{(ka)^2}{[kaj_n(ka)]'} j_n(kr), \quad (18)$$

and invoke standard Bessel function integral identities, we find the following expression for c_s

$$c_s = -\frac{2k^2}{j_n(x_{ns})} \frac{1}{(k_{ns}^2 - k^2)\left[1 - \frac{n(n+1)}{x_{ns}^2}\right]}. \quad (19)$$

Evaluating f in $r = a$ and subtracting the analogue expression for $k = k_0$, we recover the sum in (16). Therefore, we can rewrite that expression in a closed form as

$$\mathcal{Y}_{nm}^{1,1} = \frac{-1}{j\omega\mu_0 a}\left[\frac{(ka)^2 j_n(ka)}{[kaj_n(ka)]'} - \frac{(k_0 a)^2 j_n(k_0 a)}{[k_0 a j_n(k_0 a)]'}\right]. \quad (20)$$

With all elements fully defined, (12) and (15) can be solved jointly to find expressions for the unknown expansion coefficients $\alpha_{nm}^{(1)}$ and $\beta_{nm}^{(1)}$. The nonzero coefficients for the tangential electric field, for example, are given by

$$\beta_{n0}^{(1)} = \gamma_{n0}/(1 - \mathcal{Z}_n^{2,1}\mathcal{Y}_n^{1,1}). \quad (21)$$

IV. Numerical Results

To validate the analytic result obtained in the previous section, we first consider the illumination of a sphere with radius $a = 1\,\text{m}$ filled by a dielectric with relative permittivity $\epsilon_r = 10$ at a frequency of $599.584916\,\text{MHz}$ ($ka = 4\pi$), following the example in [10]. The dipole is located on the z-axis at a distance of $10\,\text{m}$ from the origin with unit dipole moment. We compare the field components on the boundary with the classic Mie series solution. Both methods employ 50 terms in their expansion which are computed using the routines of Wolfram Mathematica 12.

The $\mathbf{e}_{0,\theta}$ component on the sphere's surface is shown in Figure 2a as a function of θ and the relative error between the presented DSA-EFIE solution and the Mie series reference in Figure 2b shows machine precision agreement. The maximum relative error is of the order 10^{-12} while the average relative error equals $7.4 \cdot 10^{-14}$ (see Figure 2b). The same field component is computed for a high contrast sphere with $\epsilon = 100$ and shown on Figure 2a as well. For the same number of terms, the maximum and relative error are $3 \cdot 10^{-13}$ and 10^{-13}, respectively. The third example comprises a lossy sphere with $\epsilon_r = 10 - 5j$, for which the two relative error measures now equal $5 \cdot 10^{-13}$ and $8 \cdot 10^{-14}$ (see fig. 2b). These low error values in all three cases confirm the validity, exactness and rigor of the DSA solution.

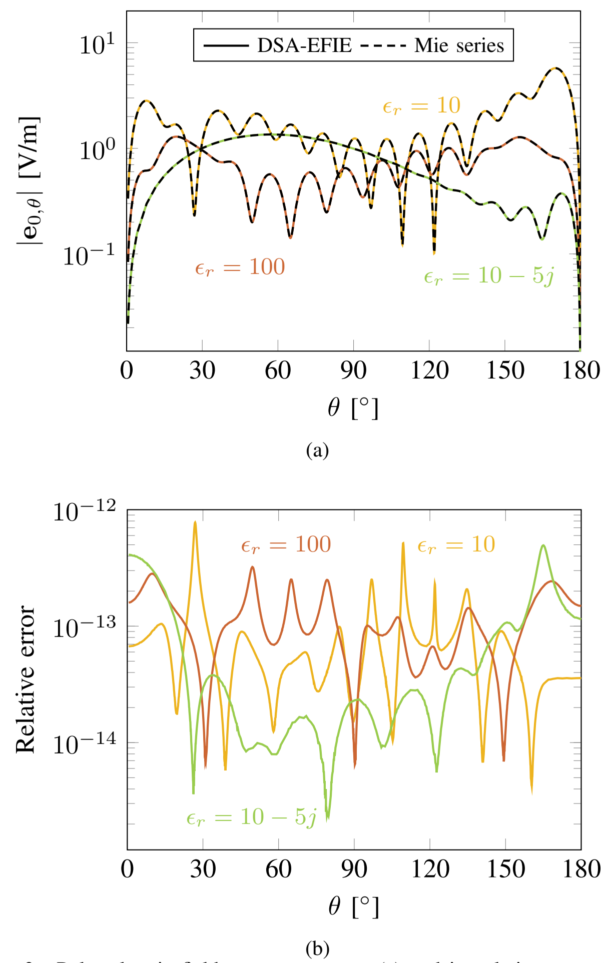

Fig. 2. Polar electric field component $\mathbf{e}_{0,\theta}$ (a) and its relative error (b) on the surface of the sphere as a function of θ. (a) The DSA result is plotted in a solid line while the Mie series reference is shown in black in dashed lines for a sphere with $\epsilon_r = 10$ (yellow), $\epsilon_r = 100$ (red) and $\epsilon_r = 10 - 5j$ (green). (b) The relative error between both solutions in (a) is plotted for all each material.

V. Conclusion

In this paper, we presented an analytical solution for scattering at a dielectric sphere using the differential surface admittance operator. Through a Galerkin approach involving vector spherical harmonics, we obtained closed expressions for the electric field integral operator governing the outside problem and the differential surface admittance operator dealing with the inside problem. For the latter, a closed sum for the infinite series involving spherical Bessel zeroes is constructed, which greatly improves the convergence of the analytical solution. A comparison with the classical Mie series showed a match of at least 12 significant digits, establishing the rigorous nature of the approach. In the future, the analysis will be extended to completion to include the tangential dipole case and a spectral analysis to determine appropriate functional spaces and frequency-dependent properties.

References

[1] D. De Zutter and L. Knockaert, "Skin effect modeling based on a differential surface admittance operator," *IEEE Trans. Microw. Theory*

Techn., vol. 53, no. 8, pp. 2526–2538, Aug. 2005.

[2] D. Bosman, M. Huynen, D. De Zutter, and D. Vande Ginste, "Construction of the differential surface admittance operator with an extended fokas method for electromagnetic scattering at polygonal objects with arbitrary material parameters," *Computers & Mathematics with Applications*, vol. 128, pp. 44–54, Dec. 2022.

[3] U. R. Patel and P. Triverio, "Skin effect modeling in conductors of arbitrary shape through a surface admittance operator and the contour integral method," *IEEE Trans. Microw. Theory Techn.*, vol. 64, no. 9, pp. 2708–2717, Sep. 2016.

[4] J. Peeters, I. Bogaert, and D. De Zutter, "Calculation of MoM interaction integrals in highly conductive media," *IEEE Trans. Antennas Propag.*, vol. 60, no. 2, pp. 930–940, Feb. 2012.

[5] T. Demeester and D. De Zutter, "Construction of the Dirichlet to Neumann boundary operator for triangles and applications in the analysis of polygonal conductors," *IEEE Trans. Microw. Theory Techn.*, vol. 58, no. 1, pp. 116–127, Jan. 2010.

[6] D. Bosman, M. Huynen, D. De Zutter, H. Rogier, and D. Vande Ginste, "A 2-D differential surface admittance operator for combined magnetic and dielectric contrast," *Computers & Mathematics with Applications*, vol. 102, pp. 175–186, Nov. 2021.

[7] M. Huynen, M. Gossye, D. De Zutter, and D. Vande Ginste, "A 3-D differential surface admittance operator for lossy dipole antenna analysis," *IEEE Antennas Wireless Propag. Lett.*, vol. 16, pp. 1052–1055, 2017.

[8] M. Huynen, K. Y. Kapusuz, X. Sun, G. Van der Plas, E. Beyne, D. De Zutter, and D. Vande Ginste, "Entire domain basis function expansion of the differential surface admittance for efficient broadband characterization of lossy interconnects," *IEEE Trans. Microw. Theory Techn.*, vol. 68, no. 4, pp. 1217–1233, 2020.

[9] G. Hsiao and R. Kleinman, "Mathematical foundations for error estimation in numerical solutions of integral equations in electromagnetics," *IEEE Trans. Antennas Propag.*, vol. 45, no. 3, pp. 316–328, 1997.

[10] O. Goni and V. I. Okhmatovski, "Analytic solution of surface–volume–surface electric field integral equation on dielectric sphere and analysis of its spectral properties," *IEEE Trans. Antennas Propag.*, vol. 69, no. 12, pp. 8479–8493, 2021.

[11] E. Martini, G. Carli, and S. Maci, "An equivalence theorem based on the use of electric currents radiating in free space," *IEEE Antennas Wireless Propag. Lett.*, vol. 7, pp. 421–424, 2008.

[12] J. G. Van Bladel, *Electromagnetic Fields*. John Wiley & Sons, Inc., May 2007.

[13] F. W. J. Olver, D. W. Lozier, R. F. Boisvert, and C. W. Clark, *NIST Handbook of Mathematical Functions*. Cambridge Univ. Press, 2010.